Bioorganic & Medicinal Chemistry 19 (2011) 4202–4210

Contents lists available at ScienceDirect

Bioorganic & Medicinal Chemistry

journal homepage: www.elsevier.com/locate/bmc

Interactions of the carrier ligands of antidiabetic metal complexes with human serum albumin: A combined spectroscopic and separation approach with molecular modeling studies

Éva A. Enyedy [a,*], László Horváth [a], Anasztázia Hetényi [b], Tiziano Tuccinardi [c], Christian G. Hartinger [d], Bernhard K. Keppler [d], Tamás Kiss [a,e,*]

[a] Department of Inorganic and Analytical Chemistry, University of Szeged, PO Box 440, H-6701 Szeged, Hungary
[b] Department of Medical Chemistry, University of Szeged, Dóm tér 8, H-6720 Szeged, Hungary
[c] Dipartimento di Scienze Farmaceutiche, Universia degli Studi di Pisa, Via Bonanno 6, I-56126 Pisa, Italy
[d] Institute of Inorganic Chemistry, University of Vienna, Waehringer Str. 42, A-1090 Vienna, Austria
[e] Bioinorganic Chemistry Research Group of the Hungarian Academy of Sciences, University of Szeged, PO Box 440, H-6701 Szeged, Hungary

ARTICLE INFO

Article history:
Received 21 April 2011
Revised 28 May 2011
Accepted 30 May 2011
Available online 21 June 2011

Keywords:
Protein–ligand interaction
Solution equilibrium
Stability constants
Fluorimetry
Site markers

ABSTRACT

The specific binding of carrier ligands of antidiabetic vanadium(IV) and zinc(II) complexes into drug binding pockets of human serum albumin (HSA) has been investigated via displacement reactions of site markers such as warfarin and dansylglycine by different spectroscopic (fluorescence, circular dichroism, NMR) and separation methods (capillary zone electrophoresis, ultrafiltration-UV). Conditional stability constants of the ligands were calculated for the binding at *sites I* and *II* of HSA. Binding *site I* was found to be the primary binding site for 2,6-pyridine dicarboxylic acid (dipic) and picolinic acid (pic), and *site II* for 6-methylpicolinic acid (6-Mepic) and maltol, although dipic, 6-Mepic and pic displace both site markers at differing extents. The experimental data is complemented by protein–ligand docking calculations for dipic and 6-Mepic which support the observations.

1. Introduction

Human serum albumin (HSA) is the most abundant serum protein (c∼42 g/L; 630 μM) of the blood and plays an important role in the transport of various endogenous and exogenous compounds. The pharmacokinetic profile and the therapeutic index of a drug is strongly affected by its binding to HSA, since this protein has influence on the free drug concentration and can solubilize poorly soluble therapeutic agents in the circulatory system which thus results in a delay of the metabolic clearance. Therefore, the albumin binding is always screened at early stages of drug discovery.[1–3] HSA has two important structurally selective drug binding pockets in subdomains IIA and IIIA, which correspond to *sites I* and *II* proposed by Sudlow.[4] Usually bulky heterocyclic compounds with a negative charge localized in the center of the molecule, such as warfarin (WF), azapropazone, phenylbutazone, etc., are found at *site I*. Binding *site II* (also called as indole-benzodiazepine site) is a hydrophobic pocket and has a high affinity for small aromatic compounds, which may be neutral or negatively charged at one end of the molecule away from the hydrophobic center. Typical ligands are ibuprofen, diazepam, L-tryptophan, etc.[1–3] However, the binding of the compounds to the binding pockets are only selective to a certain extent and some drugs interact with HSA at both sites.[1–3,5]

Similarly, in the case of metallopharmaceuticals the interaction with serum proteins has also prominent influence on the drug metabolism. Numerous antidiabetic complexes of vanadium(IV) or zinc(II), which are able to mimic physiological effects of insulin and are orally administrable, have been developed in the last decades.[6] Bis(ethylmaltolato)oxovanadium(IV) has completed phase I clinical trials and has advanced to phase II studies.[7,8] All these metal complexes are regarded as prodrugs, as their active forms differ from the administered species as a consequence of biotransformation processes in different biological milieu such the human blood

Abbreviations: 6-Mepic, 6-methylpicolinic acid; BGE, background electrolyte; BR, bilirubin; CD, circular dichroism; CMPF, 3-carboxy-4-methyl-5-propyl-2-furanpropanoic acid; CZE, capillary zone electrophoresis; D, (n-octanol-water) distribution coefficient; DG, dansylglycine; dhp, 3-hydroxy-1,2-dimethyl-pyridinone Deferiprone; dipic, 2,6-pyridine dicarboxylic acid; ε, molar absorptivity; HEPES, 4-(2-hydroxyethyl)-1-piperazineethanesulfonic acid; HMM, high molecular mass; HSA, human serum albumin; maltol, 3-hydroxy-2-methyl-4*H*-pyran-4-one; LMM, low molecular mass; P, (n-octanol-water) partition coefficient; pic, picolinic acid; STD, saturation transfer difference; WF, warfarin.

* Corresponding authors. Fax: +36 62 420505 (É.A.E.).
E-mail addresses: enyedy@chem.u-szeged.hu (É.A. Enyedy), tkiss@chem.u-szeged.hu (T. Kiss).

0968-0896/$ - see front matter © 2011 Elsevier Ltd. All rights reserved.
doi:10.1016/j.bmc.2011.05.063

serum.[6,9] Most probably the chelating ligands serve the carrier function for the metal ions and interaction with the high molecular mass serum components has a significant role in their distribution.[6,9] Transferrin is found to be the primary binder of vanadium ions under serum conditions;[10,11] while in the case of the zinc(II)-complexes HSA is by far the preferred binding partner based on CZE–ICP-MS and ultrafiltration-ICP-AES in vitro measurements.[9,12] It was also pointed out in our former works that binary interactions between HSA and the carrier ligands has influence on the distribution of both the vanadium and zinc ions in the blood serum.[9–12] The stoichiometry and conditional stability constants of the HSA complexes formed with the carrier ligands (see Scheme 1) 2,6-pyridine dicarboxylic acid (dipic), 6-methylpicolinic acid (6-Mepic), picolinic acid (pic) and 3-hydroxy-2-methyl-4*H*-pyran-4-one (maltol) were determined by ultrafiltration-UV measurements (see Table 1); on the other hand, 3-hydroxy-1,2-dimethyl-pyridinone (dhp, Deferiprone) did not exhibit measurable binding.[9] Complexes with 1:1 and 1:2 protein-to-ligand ratio are formed with dipic and 6-Mepic, and only 1:1 complexes with pic and maltol. The stability order is the following: dipic > 6-Mepic > pic > maltol.[9]

The different HSA binding abilities of these carrier ligands of antidiabetic complexes is most probably based on their various characteristics such as the lipophilicity and charge. Maltol is more lipophilic than dhp (log $D_{7.4}$: 0.09; −0.92, respectively) and 10% of maltol is deprotonated (L^-) at physiological pH, while dhp is charge-neutral (HL),[13] which may be a possible explanation for their different HSA binding. The picolinate derivatives are completely deprotonated (pic, 6-Mepic: L^-; dipic: L^{2-}) at neutral pH. Their $D_{7.4}$ value is ~0, and it is fairly difficult to compare the lipophilicity of the neutral forms of these ligands (log *P* values) due to their zwitter-ionic character and the tendency for dimerization in the case of dipic.[13] However, the comparison of the lipophilic character of their metal complexes shows that the introduction of the methyl substituent can increase significantly the lipophilicity.[13]

Besides these basic physico-chemical properties the fitting of the ligand to the binding pockets of the protein has much more important impact on the binding ability, which depends on many factors such as the ligand size, geometry and the tendency to form direct hydrogen bonds, Van der Waal and charge interactions with HSA. In order to obtain a deeper insight into the HSA binding properties of these carrier ligands (dipic, 6-Mepic, pic, maltol, dhp) at the specific drug binding sites, displacement experiments with compounds with known binding site were performed in this study by means of spectroscopic methods such as spectrofluorimetry, circular dichroism (CD) and NMR spectroscopy, and separation techniques such as ultrafiltration-UV and capillary zone electrophoresis (CZE). The anticoagulant drug WF, which is a well-known site marker often used as fluorescence probe for binding *site I* of HSA,[4,5,14–16] and dansylglycine (DG) as a *site II* marker[17–20] were used in this study (see Scheme 2). Additionally, protein–ligand docking calculations were performed to gain information about the interaction of ligands dipic and 6-Mepic into *sites I* and *II* of HSA. The entire data set is further discussed with regard to competition with the heme metabolite bilirubin (BR) also transported by HSA.[21]

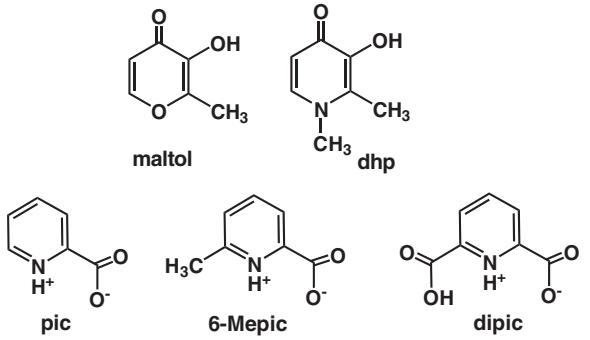

Scheme 1. Ligands used in this study in their neutral forms: maltol = 3-hydroxy-2-methyl-4*H*-pyran-4-one (HL); dhp = 3-hydroxy-1,2-dimethyl-pyridinone, Deferiprone (HL); pic = picolinic acid (HL); 6-Mepic = 6-methylpicolinic acid (HL); dipic = 2,6-pyridine dicarboxylic acid (H_2L).

Table 1
Conditional binding constants (log *K*′) and K_D values of the complexes of carrier ligands and HSA calculated from the spectrofluorimetric and ultrafiltration-UV measurements[a]

	dipic	6-Mepic	pic	maltol
Quenching[b]				
log *K*′ (PSEQUAD)	5.95(0.05)	4.60(0.02)	4.18(0.05)	n. m.[e]
K_D (PSEQUAD)	1.12 μM	25.1 μM	66.1 μM	
log *K*′ (Stern–Volmer)	5.94(0.1)	4.57(0.1)	4.29(0.1)	n. m.[e]
K_D (Stern–Volmer)	1.15 μM	26.9 μM	51.3 μM	
Site marker displacement[c]				
log *K*′(WF)	5.76(0.07)	4.42(0.09)	4.05(0.09)	n. m.[e]
log *K*′(DG)	5.23(0.1)	4.65(0.2)	3.65(0.09)	3.64(0.08)
Ultrafiltration-UV[d]				
log K'_1	6.0	5.16	4.33	3.47
log K'_2	2.9	3.12	—	—

[a] Standard deviations in parenthesis.
[b] Determined by spectrofluorimetry; {c_{HSA} = 0.8 μM; *t* = 25 °C; pH = 7.40 (2.5 mM HEPES)}.
[c] Determined by spectrofluorimetry; {c_{HSA} = 0.8 μM; $c_{site\ marker}$ = 0.8 μM; *t* = 25 °C; pH = 7.40 (2.5 mM HEPES)}; [HSA–WF]: log *K*′ = 5.79(0.01), K_D = 1.62 μM; [HSA–DG]: log *K*′ = 5.34(0.01), K_D = 4.57 μM. Data are calculated by the computer program PSEQUAD.[24]
[d] Determined by ultrafiltration-UV; data are taken from Ref. 9.
[e] Non-measurable interaction under the conditions used.

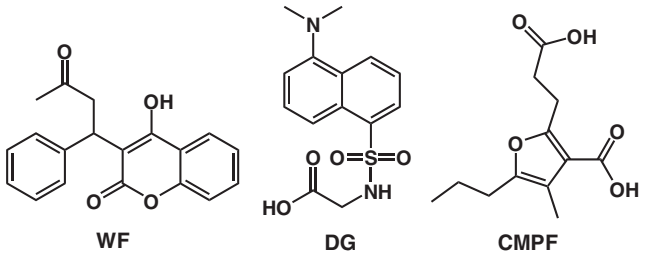

Scheme 2. Formulae of the site markers: WF = warfarin; DG = dansylglycine; and CMPF = 3-carboxy-4-methyl-5-propyl-2-furanpropanoic acid.

2. Results and discussion

2.1. Spectroscopic methods

2.1.1. Quenching and site marker displacement followed by spectrofluorimetry and CD spectroscopy

HSA exhibits significant fluorescence due to the presence of the amino acids Phe, Tyr and Trp in its primary structure.[1–3] It is well known that this protein contains a single Trp residue located in subdomain IIA (Trp214), which can be selectively excited at λ_{EX} = 295 nm. The drug binding *site I* is situated nearby Trp214 and ligand binding changes the environment of this residue, which can be detected precisely by spectrofluorimetry.[22]

It is noteworthy that the absorbance of the carrier ligands included in this study is negligible and they have no measurable emission at the excitation or emission wavelengths applied (λ_{EX} = 295, 310 and 335 nm; λ_{EM} = 310–600 nm). In this study fatty acid-containing HSA was used in order to consider the potential of HSA to bind such species in the biological environment, which can

modify the binding ability towards drugs via conformational changes at the drug binding sites.[23]

At first the reaction rate was studied. The binding of the ligands to HSA is fairly fast and the equilibrium with no further change of the emission intensity observed is reached within 5–10 min. The fluorescence quenching of Trp214 by dipic, 6-Mepic and pic is shown in Figure 1, while no measurable effect was detected in the case of addition of maltol and dhp up to tenfold excess of maltol and dhp.

The emission maximum (λ_{EM}(max) = 338 nm) was not altered significantly during the quenching. Only the binding of dipic resulted in a blue shift to 335 nm (see Fig. S1) indicating a slight decrease in the polarity of the environment of Trp214. Conditional binding constants (together with K_D dissociation constants) were calculated by the computer program PSEQUAD[24] using the whole emission wavelength range (310–400 nm) and by the Stern–Volmer linearization[25,26] at λ_{EM} = 335 nm (Table 1; for the calculation see Supplementary data). Both approaches resulted in similar binding data, although the constants obtained by the Stern–Volmer method have higher uncertainties. The order of the association constants for the binding at *site I* on HSA is the following: dipic > 6-Mepic > pic.

Prior to the displacement reactions, the interactions of the site markers DG, WF (Scheme 2) and BR with HSA were studied (for conditions see Table 2). The binding constant for WF was reported earlier under similar conditions[27] and the log *K*′[HSA–WF] value of 5.79 obtained in this study is similar and also comparable to literature data.[4,14–16] The 3D fluorescence spectra recorded for DG, HSA and an incubation mixture are shown in Figure 2. The peaks assignable to HSA (λ_{EX}(max) = 230 and 280 nm) are quenched, while that of the site marker (λ_{EX}(max) = 220 and 335 nm) are significantly increased.

Data derived from the spectra recorded for DG alone and for the HSA–DG system at various site marker concentrations (see Fig. S2), revealed a log *K*′[HSA–DG] = 5.34, which is comparable to the few binding constants available in the literature.[4,19,20] The molar intensities of DG and its HSA complex as proportional constants between intensities and concentrations are accessible by the use of PSEQUAD[24] (see Fig. 2d) whereas graphical solutions such as Stern–Volmer[25,26] and Scatchard[25,26] plots proved disadvantageous. It can be concluded that the complex [HSA–DG] is much more fluorescent than the non-bound site marker; therefore its displacement by other ligands from the binding pocket of the protein is accompanied by a considerable decrease in the emission intensity, similarly to the HSA–WF system. (It is important to note that the displacement of the site marker can be measured when the ligand binds at the binding site of the marker compound, however, when its binding constant is much lower compared to that of the site marker only a high excess of the ligand can result in a detectable effect.) Therefore, the displacement of the site markers (WF, DG) at the given binding pockets at various concentrations of the carrier ligands was followed via intensity changes of the emission spectra (as it is shown for the HSA–DG–6-Mepic system in *Fig.* S3).

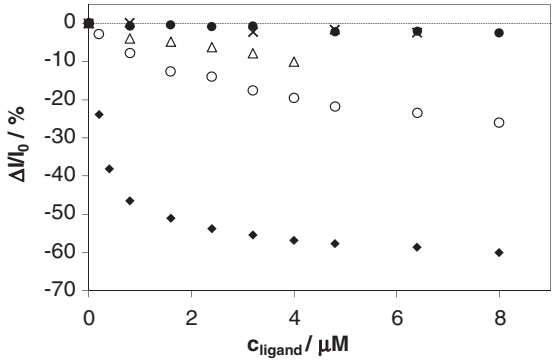

Figure 1. Changes in the emission intensities at 335 nm plotted against the concentration of dipic (♦), 6-Mepic (○), pic (Δ), maltol (●) and dhp (×) in HSA containing samples, λ_{EX} = 295 nm; λ_{EM} = 335 nm {I_0 = initial intensity when c_{ligand} = 0 M; c_{HSA} = 0.8 μM; *t* = 25 °C; pH = 7.40 (2.5 mM HEPES); PTM = 700 V; slits: 10/10 nm}.

Table 2
Conditional binding constants (log *K*′) and K_D values of the site marker–HSA complexes calculated from the spectrofluorimetric, ultrafiltration-UV and CZE measurements[a]

	WF	DG
Fluorimetry[b]		
log *K*′	5.79(0.01)	5.34(0.01)
K_D	1.62 μM	5.57 μM
Ultrafiltration-UV[c]		
log K'_1	6.08(0.02)	5.48(0.05)
log K'_2	4.22(0.06)	4.7(0.1)
log K'_3	3.7(0.10)	3.7(0.1)
CZE[d]		
log K'_1	5.0(0.1)	4.9(0.1)
log K'_2	4.0(0.1)	4.2(0.1)

[a] Standard deviations in parenthesis. Data are calculated by the computer program PSEQUAD.[24]
[b] {c_{HSA} = 0.8 μM; $c_{site\ marker}$ = 0–8 μM; *t* = 25 °C; pH = 7.40 (2.5 mM HEPES)}.
[c] {c_{HSA} = 200 μM; $c_{site\ marker}$ = 0.05–1.2 mM; *t* = 25C; pH = 7.40 (0.1 M HEPES)}.
[d] {c_{HSA} = 100 μM; $c_{site\ marker}$ = 25–800 μM; *t* = 25 °C; pH = 7.40 (20 mM phosphate buffer)}.

Binding data for the carrier ligands was calculated on the basis of the deconvolution of the emission spectra (Table 1). The ligands exhibit different readiness to compete with WF and DG for the binding *sites I* and *II* (see Figs. 3, S4 and 5). The intensity changes are compared to the maximal changes of the complete displacement at 1:1:5 protein-to-site marker-to-ligand ratio in Figure 4. All these findings show that dipic, 6-Mepic and pic are able to compete with WF efficiently and in that order, whereas measurable displacement of DG takes place in the sequence of dipic > 6-Mepic > pic ≈ maltol. Most probably dipic, 6-Mepic and pic are able to attach to both binding sites, while maltol shows minor affinity only to *site II*. Thus, *site I* is identified as the primary binding site of dipic and pic and *site II* for 6-Mepic and maltol, and dhp does not interact with HSA.

In addition to DG and WF, BR was used as a selective site marker for *site I* of HSA. BR is a relatively strong HSA binder, with a negligible intrinsic emission, while its protein complex [HSA–BR] emits moderately at λ_{EX} = 487 nm. A log *K*′[HSA–BR] value of 7.30(0.01) was calculated based on the emission spectra recorded for the HSA–BR system, following the self-absorbance correction of the measured intensities[25,26] due to the considerable absorbance of the samples. The values found in the literature spread widely and are between 6.5 and 8.0.[21,28,29] When adding dipic at high excess, a decrease of the emission intensity in the HSA–BR–dipic system was measured, and this finding corresponds well to the concentration distribution curves calculated with the help of the stability constants of complexes [HSA–BR] and [HSA–dipic] (see Fig. S6).

BR and its complex formed with HSA are optically active and their CD spectra show quite different character (Fig. 4). Thus, the decrease of the ΔAbsorbance at 442 and 474 nm is unambiguously related to the partial displacement of BR by dipic, but it is observed only when high excess of the ligand is used. Dipic is supposed to compete with BR most efficiently as it is the strongest binder among the carrier ligands studied; and these results show that this competition may have some importance under realistic conditions.

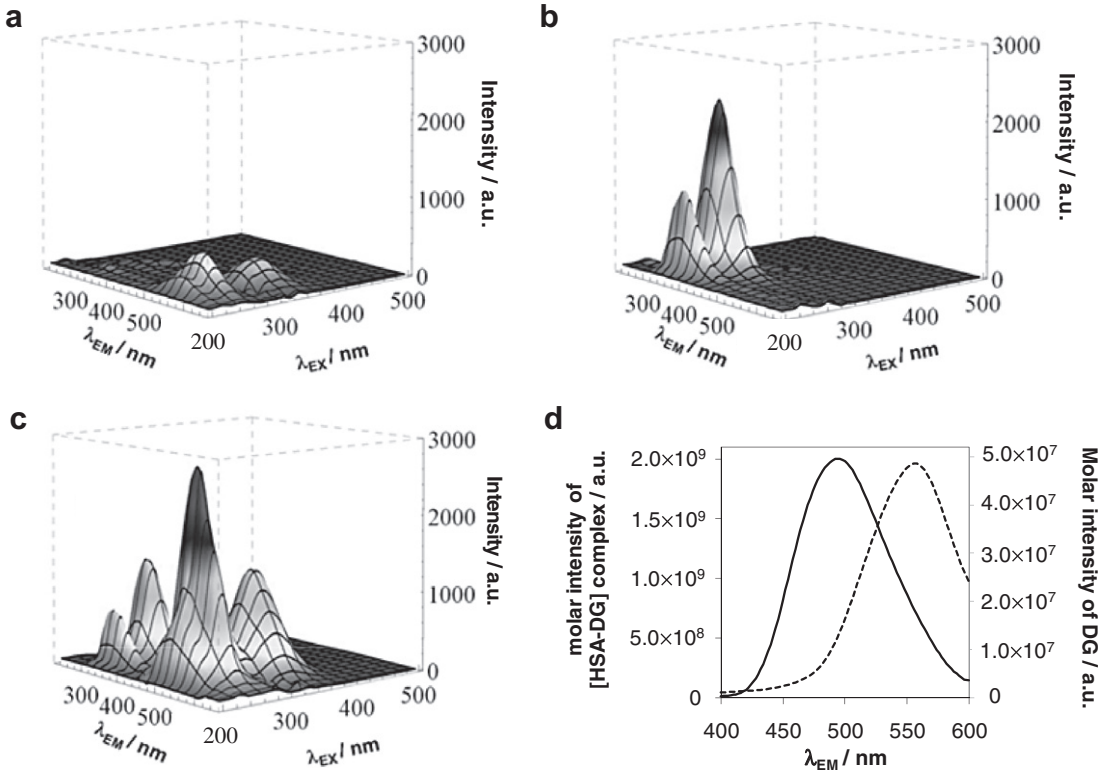

Figure 2. 3D fluorescence spectra of 10 μM DG (a), 1 μM HSA (b) 1 μM HSA–10 μM DG (1:10) (c) samples. Molar fluorescence emission spectra of DG (dashed line) and the [HSA–DG] complex (solid line) at λ_{EX} = 335 nm (d) {t = 25 °C; pH = 7.40 (2.5 mM HEPES); PTM = 700 V; slits: 10/10 nm}.

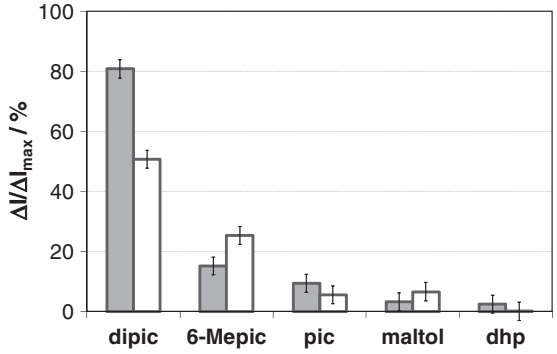

Figure 3. Changes in the emission intensities in samples of HSA–WF–ligand (1:1:5) (gray bar, λ_{EX} = 310 nm, λ_{EM} = 390 nm) and HSA–DG–ligand (1:1:5) (white bar, λ_{EX} = 335 nm, λ_{EM} = 496 nm), when ΔI_{max} is the maximal change at the complete displacement of the site marker {c_{HSA} = 0.8 μM; t = 25 °C; pH = 7.40 (2.5 mM HEPES); PTM = 700 V; slits: 10/10 nm}.

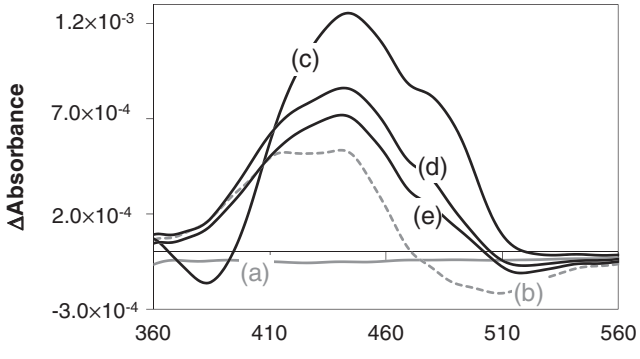

Figure 4. CD spectra of HSA (a), BR (b), HSA–BR (1:2) (c), HSA–BR–dipic (1:2:20) (d), HSA–BR–dipic (1:2:40) (e) {c_{HSA} = 20 μM; c_{BR} = 40 μM; c_{dipic} = 0–0.8 mM; t = 25 °C; pH = 7.40 (30 mM HEPES)}.

2.1.2. Direct binding and site marker displacement studies by NMR spectroscopic methods

NMR spectroscopy is a useful technique for studying dynamic protein–ligand interactions, because structural information is obtained non-invasively without requiring separation. In order to elucidate the binding of the ligands towards HSA, saturation transfer difference (STD) NMR spectroscopy measurements were performed. In such an experiment the binding of a smaller molecule to the protein with a conditional binding constants log K'∼3–8 causes the saturation also to spread onto the ligand and the intensity of the ligand signal will be attenuated.[30] Subtraction of this spectrum from the reference spectrum of the ligand without saturation results in the STD NMR spectrum and therefore, only binder ligand molecules exhibit STD NMR spectra. This kind of NMR spectroscopy enables the identification of ligand binding to proteins when the intermediate exchange on the chemical-shift time scale is fast.[30] 'Exchange' here relates to the exchange between free and bound states of the ligand.

Individual ^{1}H NMR spectra of dipic, 6-Mepic, maltol, pic and dhp were recorded in phosphate buffer at pH 7.4 and compared to a mixture of all ligands in a single sample. All signals were distinguishable in the latter sample (Fig. S7). Thus, an equimolar mixture of the ligands was used in the STD NMR experiments. The STD signals measured for the HSA–ligand samples corroborate the existence of the binding between HSA and ligands dipic, 6-Mepic, maltol and pic, but dhp seems do not bind due to the lack of its CH_3 signal at 3.7 ppm (see Fig. 5).

Furthermore, the competition with WF and DG site markers were studied and the effect of the binding WF or DG ligand to

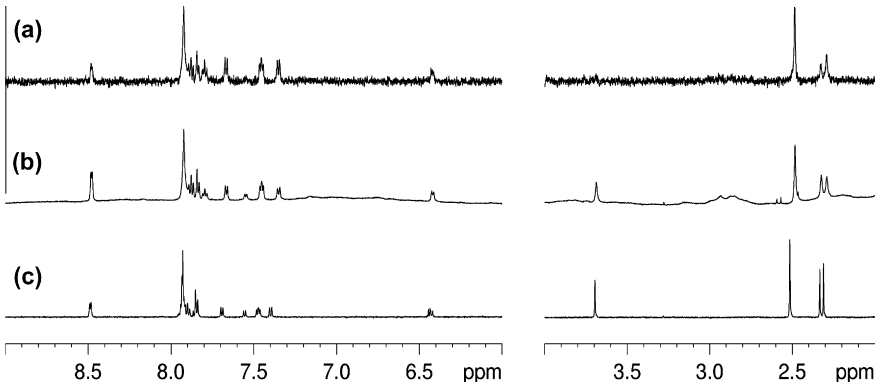

Figure 5. STD NMR spectra obtained for HSA and the ligands pre-incubated for 30 min (a); ^{1}H NMR spectra of HSA and the ligands (b); ^{1}H NMR spectra of the ligands (c).

HSA was examined at a 1:1 protein-to-site marker ratio. No STD signals were detected for WF, most probably due to the slow ligand exchange on the NMR time scale. Practically the entire amount of WF was found attached to HSA and almost no free WF signal was visible in the ^{1}H NMR of an HSA–WF sample (see Fig. S8). Equimolar mixtures of the carrier ligands were co-incubated with an HSA–WF sample (see Fig. 6.a, b). Only weak STD signals were observed, which are similar to the resonances observed for the HSA–ligand samples (Fig. 5a). This finding also supports that the ligands can compete for the binding pocket, even at slow exchange between free and bound WF. When doubling the amounts of dipic and 6-Mepic in the samples, stronger STD signals were observed (Fig. 6c, d).

STD NMR spectra obtained for the HSA–DG sample revealed an expectable behavior for this site marker in presence of the protein (*Fig.* S9). In order to the study a competitive behavior, the ligands were added to the co-incubated HSA–DG sample and STD signals of the carrier ligands were observed. These signals were weaker than in absence of the site marker underlining that some of the ligands have affinity for the same binding pocket as DG, that is, *site II* (see Fig. S10).

2.2. Separation methods: membrane ultrafiltration-UV and CZE-UV

In addition to the spectroscopic studies, the competition of the carrier ligands for the HSA binding sites with WF and DG was studied by means of ultrafiltration-UV and CZE-UV. The direct interaction between these site markers and HSA was examined by ultrafiltration-UV experiments, using mixtures of HSA and WF or DG at different ratios. The non-bound fraction was separated from HSA and the HSA-site marker complexes, which were collected in the high molecular mass (HMM) fraction. Then UV spectra of the low molecular mass (LMM) fractions compared to reference spectra were analyzed (see Fig. S11 for the HSA–DG system), and the ratios of the non-bound and total amount of the compounds were obtained. From these data pairs (see Fig. S12), the stoichiometry and conditional stability constants of the HSA complexes were calculated (Table 2). Similarly, the concentration of the non-bound site marker was determined by CZE (see Figs. 7 and S13), when various molar ratios of HSA-to-site marker were used. Sufficient separation of proteinaceous species from free site marker was achieved. High specificity for the site markers was observed at detection wavelengths of 320 and 330 nm, where only WF or DG absorbs, respectively, but not HSA.

For quantification of the binding extent of the site markers, external calibration curves were determined under identical CZE conditions (see Figs. S14 and 15). Based on the collected data set, conditional stability constants were calculated (see Supplementary data), which are listed in Table 2. Whilst only the first stepwise stability constants could be determined in the case of the spectrofluorimetry due to the highly diluted conditions, the binding data for the second (and third, which is quite uncertain) steps were obtained by applying the separation techniques. Comparing the $\log K'_1$ values calculated by the different methods it can be seen that ultrafiltration-UV gave somewhat higher and CZE slightly lower values than spectrofluorimetry. These discrepancies can be explained by the slightly different experimental conditions. Furthermore, separation approaches may affect the equilibrium state and therefore, the displacement processes of the site markers by

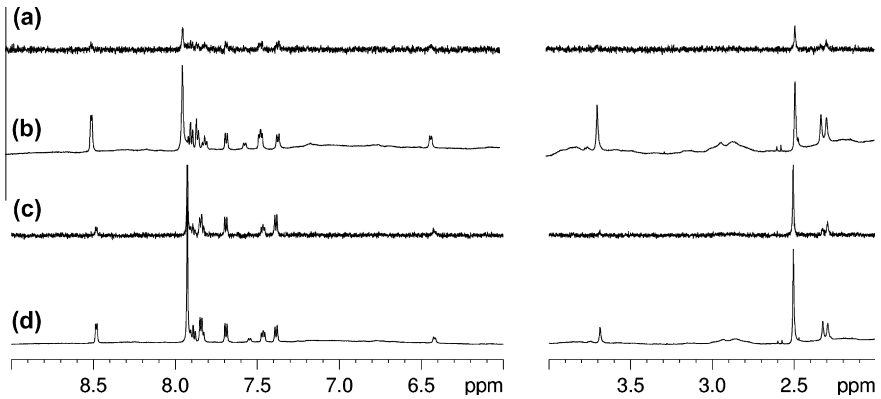

Figure 6. STD NMR spectra obtained for HSA–WF–ligands sample (HSA–WF–dipic–6-Mepic–pic–maltol–dhp = 1:1:5:5:5:5:5) (a) or 1:1:10:10:5:5:5 (c); ^{1}H NMR spectra of HSA–WF–ligands sample (HSA–WF–dipic–6-Mepic–pic–maltol–dhp = 1:1:5:5:5:5:5) (b) or 1:1:10:10:5:5:5 (d).

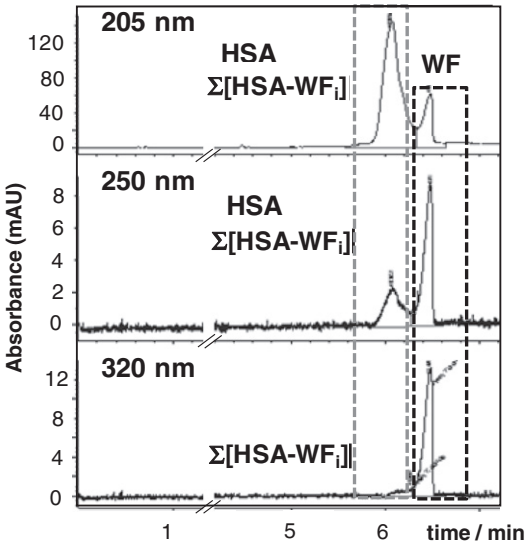

Figure 7. Representative electropherograms for the HSA–WF system at various wavelengths {c_{HSA} = 100 μM, c_{WF} = 500 μM, t = 25 °C; pH = 7.4 (phosphate buffer (20 mM)}.

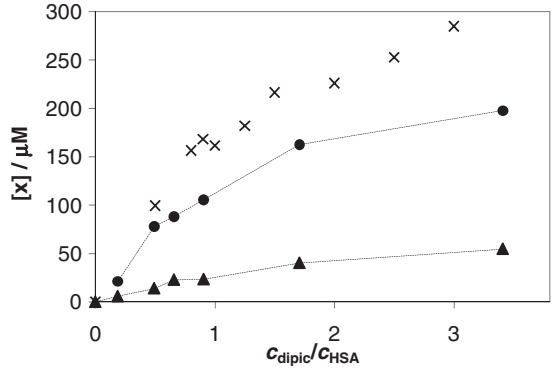

Figure 8. Equilibrium concentrations of the bound dipic (●); WF displaced by dipic (▲) in the HSA–WF–dipic system; and those of bound dipic in absence of WF (×) obtained by ultrafiltration-UV. {Original sample composition: c_{HSA} = 200 μM; c_{WF} = 200 or 0 μM; c_{dipic} = 37–682 μM; pH = 7.4 (HEPES (0.10 M); t = 25 °C}.

the carrier ligands were considered mostly qualitatively in the case of the ultrafiltration-UV and CZE methods. Thus, binding constants were not calculated for the additional species possibly formed under the conditions of the separation methods, such as the ternary complexes [HSA–WF–dipic] and [HSA–DG–6-Mepic] etc.

In order to determine the displacement capacity of the site markers by dipic, 6-Mepic, pic and maltol, ultrafiltration and CZE studies of the ternary systems were carried out. Ultrafiltration of mixtures containing HSA and site markers at a ratio of 1:1 as well as the carrier ligands in different concentrations resulted in LMM and HMM fractions. UV spectra of the LMM fractions of the ternary HSA-site marker-ligand systems following the ultrafiltration were recorded (Fig. S16) and compared to those containing no ligands. Then the equilibrium concentration of the non-bound site marker and ligand was calculated by the deconvolution of these spectra on the basis of the molar absorbance spectra of the compounds (see Fig. S17). For the HSA–WF–dipic system (Fig. 8) the concentration of the bound dipic is increased with higher HSA(WF)-to-dipic ratio, but it is always lower than the values measured in absence of WF and is much higher than the concentration of the WF displaced. This finding shows that there is a competition for binding *site I* between WF and dipic, but dipic is able to bind at the other binding

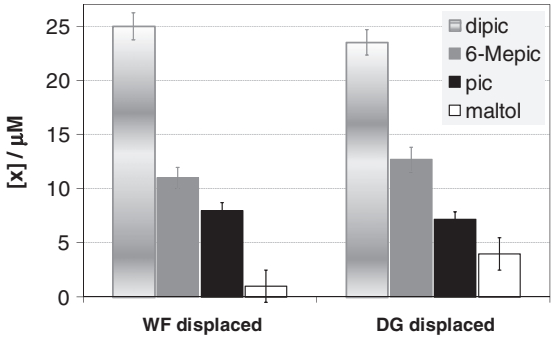

Figure 9. Equilibrium concentrations of the site markers displaced by the ligands in HSA–site marker–ligand (1:1:1) systems in the LMM fractions after separation obtained by ultrafiltration-UV. {Original sample composition: c_{HSA} = 200 μM; pH = 7.4 (HEPES (0.10 M); t = 25 °C}.

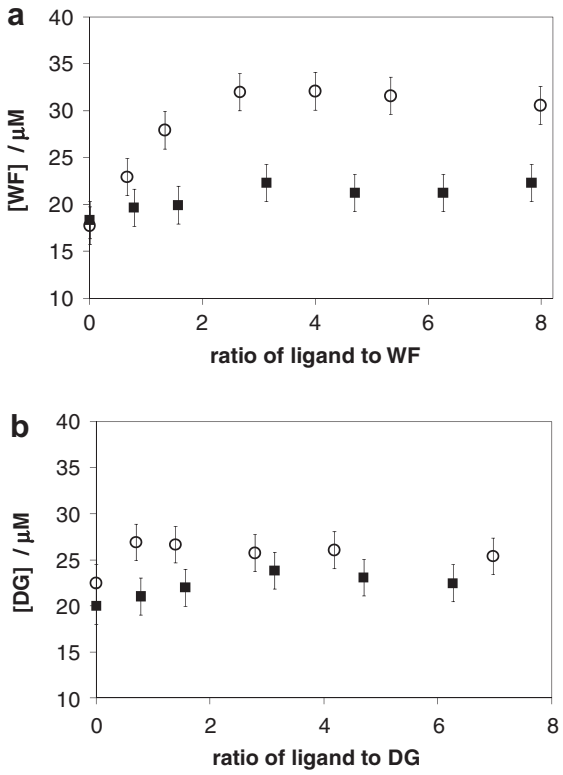

Figure 10. Changes of the equilibrium concentrations of the non-bound site marker (WF (a), DG (b)) in the HSA–site marker–dipic (○) or HSA–site marker–6-Mepic (■) systems at various ligand ratios obtained by CZE. {c_{HSA} = 100 μM; c_{WF} = 100 μM; c_{ligand} = 0–800 μM; pH = 7.4 (20 mM phosphate buffer); t = 25 °C}.

pocket as well. Thus, formation of mixed ligand species such as [HSA–WF–dipic] is probable. The amounts of displaced site markers (WF, DG) are compared for the various ligands in Figure 9. It can be seen that WF is substituted by the ligands in the order of dipic > 6-Mepic > pic, whereas the effect of maltol is negligible. A similar order was observed for DG, but the concentration of the site marker displaced by maltol and 6-Mepic is somewhat higher than in case of WF.

In the corresponding CZE experiments only the changes in the concentration of the free (non-bound) site marker could be monitored. The total concentration of dipic and 6-Mepic was varied keeping the ratio of the HSA-to-site marker constant and the results are shown in Figure 10. The increasing amount of the non-bound site marker with increasing ligand concentrations revealed

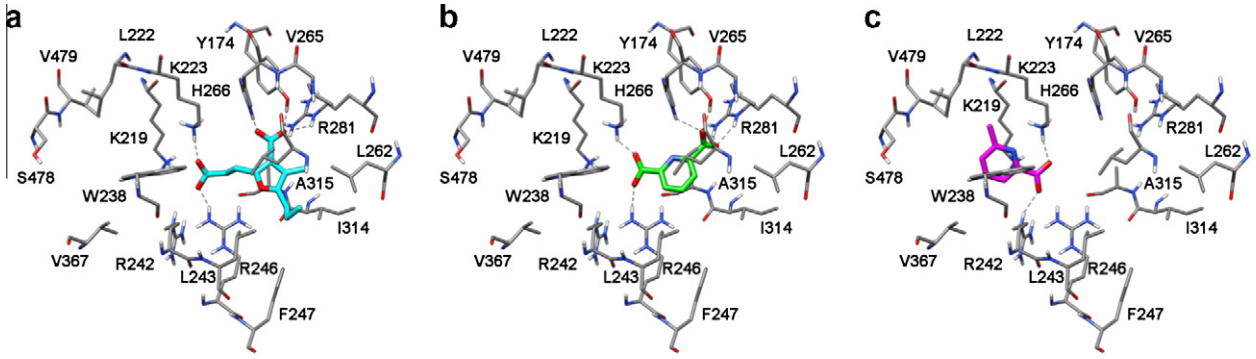

Figure 11. Docking of compounds into *site I* of HSA: CMPF (a); dipic (b); 6-Mepic (c).

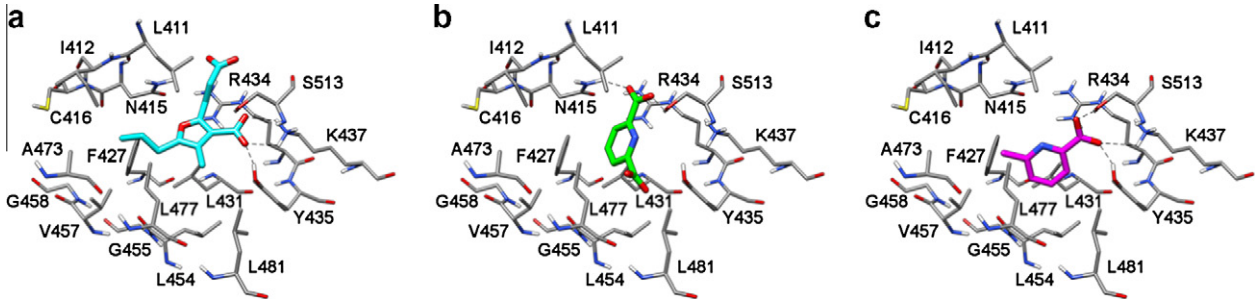

Figure 12. Docking of compounds into *site II* of HSA: CMPF (a); dipic (b); 6-Mepic (c).

that these carrier ligands tend to compete for the HSA binding sites with WF and DG. However, only the displacement of WF by dipic is remarkable under the applied conditions. The amount of the displaced WF or DG is higher with dipic compared to 6-Mepic. The difference between the effect of dipic and 6-Mepic is much smaller in the case of DG as observed with the other methods (Fig. 9 or cf. Figs. S4 and 5).

However, based on these findings similar conclusions can be drawn as from the spectroscopic studies (see Section 2.1.1); namely, the ligands dipic, 6-Mepic and pic have a tendency to interact with the HSA at the binding sites of both WF and DG but maltol binds most probably exclusively at *site II*. The WF binding site is more favorable for dipic and pic, whereas 6-Mepic slightly prefers *site II* over *site I*.

2.3. Docking calculations

To investigate the binding interactions between the analyzed compounds and the HSA and in particular to characterize their different affinity for the two main binding sites of the protein, an automated docking procedure using the software GOLD[31] was applied to dipic and 6-Mepic. The binding disposition of 3-carboxy-4-methyl-5-propyl-2-furanpropanoic acid (CMPF, see Scheme 2) towards HSA was used as a reference, as an X-ray structure of the HSA–CMPF complex confirms that this compound is able to interact with both *site I* and *site II* of the protein.[32]

Dipic and 6-Mepic were docked into both binding sites of HSA. At *site I*, the 3-carboxylate group of CMPF interacts with Tyr174, His266 and Arg281 (Fig. 11a), while the carboxyethyl group forms H-bonds with Lys223 and Arg246. The *n*-propyl substituent is located in the lipophilic pocket mainly delimited by Leu243, Phe247, Leu262 and Ile314. As shown in Figure 11b, the binding interactions of dipic were very similar to those of CMPF at *site I* with the two carboxylate functionalities interacting, as in case of CMPF, with Tyr174, Lys223, Arg246, His266 and Arg281. Interestingly, the substitution of one of the two carboxylates with a methyl group, causes a completely different binding disposition (see Fig. 11 c), with the carboxylic acid group interacting with Lys223 and Arg246 while the methyl group is found in a pocket close to Leu222.

At *site II*, the 3-carboxylic group of CMPF interacts with Tyr435 and Lys437 (Fig. 12a), the propanoic acid group is exposed to the solvent and the *n*-propyl chain binds into a lipophilic pocket created by Ile412, Phe427, Val457 and Leu477. In the case of dipic, one of the two carboxylic acid groups forms H-bonds with Asn415 and Ser513 (Fig. 12b), while the other carboxylate does not show important interactions. In contrast to dipic, 6-Mepic shows a binding disposition very similar to that of CMPF at *site II*, with the carboxylic acid interacting with Tyr435, Lys437and Ser513 and the methyl substituent with a lipophilic pocket delimited by Ile412, Phe427, Val457 and Leu477 (see Fig. 12c).

The comparison of in silico data on the interactions of the two carrier ligands dipic and 6-Mepic with the HSA binding sites highlights that (i) dipic shows stronger binding into *site I* since, differently from *site II*, both carboxylic functions are involved in H-bonds; (ii) the carboxylate of 6-Mepic forms H-bonds with amino acid residues in both binding sites, but the methyl substituent showed somewhat stronger lipophilic interactions at *site II*. Therefore, the docking results support the hypothesis that the primary binding site of dipic is *site I*, while the interaction of 6-Mepic with *site II* is more favorable.

3. Conclusions

A panel of methods comprising spectrofluorimetry, CD and ^{1}H NMR spectroscopy, membrane ultrafiltration-UV and CZE in addition to in silico calculations was used to study the interactions of the ligands dipic, 6-Mepic, pic, maltol and dhp with HSA, which has considerable effect on the biodistribution of antidiabetic zinc(II) and vanadium(IV) complexes in the human blood serum. Binding properties at the specific binding pockets of the protein were measured with the help of site markers such as WF, DG

and BR by displacement experiments. The data show that considerable displacement of WF takes place upon addition of dipic, 6-Mepic and pic (in this order), showing that these ligands can bind at *site I* of HSA. At the same time they are also able to displace DG at *site II* to some extent. *Site I* is most likely the primary binding site for dipic and pic, whereas *site II* is more favorable for 6-Mepic due to lipophilic interactions between this ligand and the binding pocket of HSA in the subdomain IIIA. Moreover, a weak binding of maltol appears at *site II*, and the charge-neutral dhp does not seem to displace any site marker from the respective HSA binding sites. Measurable competition with BR can only take place with the strongest binder, that is, dipic, at rather high ligand excess. The application of different complementary techniques with their advantages and disadvantages can contribute to a more complete understanding of specific protein–ligand interactions.

Now, the next question arises, whether the ligands can carry metal ions as well when bind to the specific sites of HSA or the metal complexes or metal ions (vanadium and/or zinc) are carried in different sites. Studies to answer this question are undergoing in our laboratories.

4. Experimental

4.1. Chemicals

Maltol, dhp, pic, 6-Mepic, dipic, racemic WF, DG, BR, HSA (as lyophilized powder with fatty acids), 4-(2-hydroxyethyl)-1-piperazineethanesulfonic acid (HEPES), KH_2PO_4 and K_2HPO_4 were commercially available products of *puriss* quality (Sigma–Aldrich). Doubly-distilled Milli-Q water was used for sample preparations. The purity of the carrier ligands was checked and the exact concentrations of the stock solutions prepared were determined by potentiometric titrations using the program SUPERQUAD for data evaluation.[33]

HSA solutions were always prepared freshly and their concentrations were estimated from the UV absorption: ε_{280nm}(HSA) = 36850 M^{-1} cm^{-1}.[34] Solutions of WF and DG were prepared prior to the measurements with one equivalent of NaOH in HEPES or phosphate buffers at pH 7.40. Their concentrations were calculated on the basis of their UV spectra: ε_{308nm}(WF) = 14475 M^{-1} cm^{-1}, ε_{327nm}(DG) = 5068 M^{-1} cm^{-1}.

4.2. Spectrofluorimetric and CD spectroscopic measurements

Fluorescence spectra were recorded with a Hitachi-F4500 fluorimeter using 10 nm/10 nm slit width in 1 cm quartz cells at 25.0 ± 0.1 °C. All solutions were prepared in 2.5 mM HEPES at pH 7.40. Samples usually contained 0.8 μM HSA and varying HSA-to-ligand ratios (1:0–1:22). In the site marker displacement experiments, the HSA-to-site marker (WF, DG or BR) ratio was always 1:1 and the concentration of the carrier ligand (maltol, dhp, pic, 6-Mepic, dipic) was varied. Spectra were recorded after 10 min incubation time. BR-containing samples were kept in the dark. The excitation wavelength was 295, 310, 335 or 487 nm depending on the type of the experiment and the emission was read in the range of 310–700 nm (see the details in Supplementary data). The conditional binding constants were then calculated with the computer program PSEQUAD[24] and quenching data were also analyzed by the Stern–Volmer equation[25,26] for comparison (see Supplementary data).

Three-dimensional spectra were recorded at 200–500 nm excitations, and at 250–600 nm emission wavelengths.

CD spectra were recorded on a Jobin-Yvon Mark VI dichrograph in the wavelength range from 300 to 3600 nm, in an optical cell of 1 cm path length at 25 °C. The analytical concentration of HSA was 20 μM, and HSA-to-BR-to-dipic ratios were 1:0:0, 0:2:0, 1:2:0, 1:2:20, 1:2:40 in 30 mM HEPES buffer at pH 7.40. Samples were incubated for 10 min in the dark.

4.3. NMR measurements

All NMR spectra were recorded on a Bruker AV600 spectrometer equipped with a 2.5-mm triple-resonance capillary probe at a temperature of 25 °C. The ^{1}H NMR measurements were performed with a WATERGATE solvent suppression scheme. All samples were measured with the same experimental parameters, the same spectrometer and the same probe. For the relaxation delay, 2 s was used; the delay for binomial water suppression was 150 μs; the number of scans was 256.

STD NMR measurements were performed with the WATERGATE water suppression pulse scheme. The irradiation power was 20 Hz, which was applied on-resonance at 0 ppm and off-resonance at 40 ppm. A total of 512 scans were accumulated for each pseudo 2D experiment, resulting in a total experiment time of 2 h.

All NMR spectra were processed and analyzed with Topspin 2.0 (Bruker) so that line-width effects on the intensity of the signal were negligible. Extreme care was taken to scale the measured signal intensities properly with respect to the slightly different concentrations in the reference spectra and the final HSA samples. All the measurements were repeated at least three times on separate samples, and the reproducibility of the bound fractions were within a relative error of 2%.

10 mM stock solutions of the carrier ligands were prepared in 20 mM phosphate 90:10 H_2O/D_2O buffer at pH 7.4. First, 15 μl ligand stock solution and 120 μl buffer were mixed and transferred to a 2.5 mm capillary NMR tube and the reference ^{1}H NMR spectrum was recorded. Subsequently, 15 μl 2 mM HSA stock solution was transferred into the NMR tube and the mixture was allowed to stand for 30 min to facilitate the equilibrium state. In the final sample, the HSA-to-ligand ratio was 1:5. For the competition measurements, 15 μl 2 mM stock solution of WF or DG and 15 μl 2 mM stock solution of HSA and 45 μl 20 mM phosphate 90:10 H_2O/D_2O buffer at pH 7.4 were co-incubated for 30 min. Subsequently, the ligands were added as 15 μl stock solution, respectively, to the existing sample.

4.4. Membrane ultrafiltration-UV measurements

Samples were separated by ultrafiltration through 10 kDa membrane filters (Microcon YM-10 centrifugal filter unit, Millipore). All 0.50 ml samples contained 200 μM HSA and the ligands (from 50 μM to 1.2 mM) in 0.10 M HEPES buffer at pH 7.40 at 25.0 ± 0.1 °C and were incubated for 1 h. In the site marker displacement experiments the HSA-to-site marker ratio was always 1:1 and the concentration of the carrier ligand was varied. Then the low molecular mass (LMM) fractions containing the non-bound ligands were separated from HSA and HSA–ligand complexes in the high molecular mass (HMM) fractions with the help of a temperature controlled centrifuge (Sanyo, 10000/s, 45–50 min). The LMM fractions were diluted to 5.00 ml and the concentrations of the non-bound ligand were determined by UV spectrophotometry. The UV spectra of the LMM fractions were always compared with the reference spectra of the samples containing the ligand without protein in an analytical concentration equal to that in the ultrafiltered samples. An Unicam Helios Alpha spectrophotometer was used to record the spectra in the region of 250–400 nm at 25 °C and with a path length of 1 cm.

Stoichiometries and conditional binding constants (log β′) were then calculated based on the equilibrium processes and mass-balance equations for the components (see Supplementary data) with the computer program PSEQUAD[24] from the total and protein-free

concentration data pairs of the ligands obtained at different protein-to-ligand ratios; uncertainties in the stability constants are given in parentheses.

4.5. CZE measurements

CZE experiments were performed with an HP^{3D} CZE system (Agilent Technologies). For all experiments capillaries of 60 cm total length (50 μm ID) were used (BGB Analytik AG). The detection was carried out by on-column UV photometric measurement in the range of 200–330 nm. Injections were performed by applying a pressure of 25 mbar for 5 s, and constant voltages of 28 kV were used for phosphate buffer at pH 7.40 as background electrolyte (BGE). Prior to the first use, the capillary was flushed at 1 bar with 0.1 M HCl, water, 0.1 M NaOH and again with water (10 min each). Before each injection, the capillary was purged for 2 min both with water and the BGE followed by applying a voltage of 28 kV for 30 s and flushed for 1 min with BGE again. The cleaning procedure included purging with 0.1 M HCl, water and 0.1 M NaOH (each for 2 min). The CZE data was recorded using the ChemStation software (HP, Agilent Technologies). Stoichiometries and conditional binding constants were calculated with the computer program PSEQUAD[24] (see Supplementary data).

Samples containing 100 μM HSA and the ligands (from 25 to 800 μM) in 20 mM phosphate buffer at pH 7.40 and 25.0 ± 0.1 °C were incubated for 1 h prior to the measurements. (The use of HEPES buffer for the CZE runs was avoided due to its high absorption in the UV range.) In the WF or DG displacement experiments the HSA-to-site marker ratio was always 1:1 and the concentration of dipic and 6-Mepic was varied. The peak height and area of the non-bound site marker were used in order to obtain its concentration and an external calibration in the concentration range of 30–355 μM was used for determining the linear relationship between them under the conditions.

4.6. Docking of dipic and 6-Mepic with HSA

The X-ray structure of HSA complexed with CMPF[32] (PDB code 2BXA) was taken from the Protein Data Bank.[35] The ligands were built using Maestro 9.0[36] and were minimized using the conjugate gradient method until a convergence value of 0.05 kcal/mol × Å was reached. The minimization was carried out in a water environment model (generalized-Born/surface-area model) using the MMFFs force field and a distance-dependent dielectric constant of 1.0. Automated docking was carried out by means of the GOLD program, version 4.1.1.[31] The region of interest used by GOLD was defined in order to contain the residues within 10 Å from the original position of CMPF into (i) *site I* and (ii) *site II* in the X-ray structures. The 'allow early termination' option was deactivated, the remaining GOLD default parameters were used, and the ligands were submitted to 50 genetic algorithm runs by applying the ChemScore fitness function. The best docked conformation was taken into account.

Acknowledgments

This work has been supported by the Hungarian Research Foundation OTKA K77833, PD 83600. 'TÁMOP-4.2.1/B-09/1/KONV-2010-0005–Creating the Center of Excellence at the University of Szeged' is supported by the European Union and co-financed by the European RegionalFund. É.A.E. and A.H. gratefully acknowledge the financial support of J. Bolyai research fellowship. We thank Ms. Orsolya Dömötör for performing some spectrofluorimetric studies.

Supplementary data

Supplementary data associated with this article can be found, in the online version, at doi:10.1016/j.bmc.2011.05.063.

References and notes

1. Kragh-Hansen, U. *Pharmacol. Rev.* **1994**, *33*, 17.
2. Day, Y. S. N.; Myszka, D. G. *J. Pharm. Sci.* **2003**, *92*, 333.
3. Tajmir-Riahi, H. A. *Scientica Iranica* **2007**, *14*, 87.
4. Sudlow, G.; Birkett, D. J.; Wade, D. N. *Mol. Pharmacol.* **1975**, *11*, 824.
5. Buttar, D.; Colclough, N.; Gerhardt, S.; MacFaul, P. A.; Phillips, S. D.; Plowright, A.; Whittamore, P.; Tam, K.; Maskos, K.; Steinbacher, S.; Steuber, H. *Bioorg. Med. Chem.* **2010**, *18*, 7486.
6. Thompson, K. H. *Book of Abstracts, Sixth International Vanadium Symposium* **2008**, Lisbon.
7. Thompson, K. H.; Barta, C. A.; Orvig, C. *Chem. Soc. Rev.* **2006**, *35*, 545.
8. Kiss, T.; Jakusch, T.; Hollender, D.; Dörnyei, A.; Enyedy, E. A.; Costa Pessoa, J.; Sakurai, H.; Sanz-Medel, A. *Coord. Chem. Rev.* **2008**, *252*, 1153.
9. Kiss, T.; Jakusch, T.; Hollender, D.; Enyedy, E. A.; Horváth, L. *J. Inorg. Biochem.* **2009**, *103*, 527.
10. Jakusch, T.; Hollender, D.; Enyedy, É. A.; González, C. S.; Montes-Bayón, M.; Sanz Medel, A.; Costa Pessoa, J.; Tomaz, I.; Kiss, T. *Dalton Trans.* **2009**, 2428.
11. Jakusch, T.; Costa Pessoa, J.; Kiss, T. *Coord. Chem. Rev.* **2011**. doi:10.1016/j.ccr.2011.02.022.
12. Bytzek, A. K.; Enyedy, E. A.; Kiss, T.; Keppler, B. K.; Hartinger, C. G. *Electrophoresis* **2009**, *30*, 4075.
13. Enyedy, E. A.; Hollender, D.; Kiss, T. *J. Pharmaceutical. Biomed. Anal.* **2011**, *54*, 1073.
14. Epps, D. E.; Raub, T. J.; Kézdy, F. J. *Anal. Biochem.* **1995**, *227*, 342.
15. Pinkerton, T. C.; Koeplinger, K. A. *Anal. Chem.* **1990**, *62*, 2114.
16. Wilting, J.; van der Giesen, W. F.; Janssen, L. H. M.; Weideman, M. M.; Otagirig, M. *J. Biol. Chem.* **1980**, *255*, 3032.
17. Muller, N.; Lapicque, F.; Drelon, E.; Netter, P. *J. Pharm. Pharmacol.* **1994**, *46*, 300.
18. Lucas, L. H.; Price, K. E.; Larive, C. K. *J. Am. Chem. Soc.* **2004**, *126*, 14258.
19. Hutchinson, J. P.; Oldham, T. C.; El-Thaher, T. S. H.; Miller, A. D. *J. Chem. Soc., Perkin Trans. 2* **1997**, 279.
20. Chignell, C. F. *Mol. Pharmacol.* **1969**, *5*, 244.
21. Brodersen, R. Physical Chemistry of Bilirubin: binding to Macromolecules and Membranes. In *Bilirubin*; Heirwegh, K. P. M., Brown, S. B., Eds.; CRC Press: Florida, Boca Raton, 1982; pp 75–123.
22. Eftink, M. R.; Ghiron, C. A. *Anal. Biochem.* **1980**, *114*, 199.
23. Fasano, M.; Curry, S.; Terreno, E.; Galliano, M.; Fanali, G.; Narciso, P.; Notari, S.; Ascenzi, P. *IUBMB Life* **2005**, *57*, 787.
24. Zékány, L.; Nagypál, I. In *Computational Methods for the Determination of Stability Constants*; Leggett, D. L., Ed.; Plenum Press: New York, 1985; pp 291–353.
25. Lakowicz, J. R. *Principles of Fluorescence Spectroscopy*; Plenum Press: New York, 1983.
26. Valeur, B. *Molecular Fluorescence Principles and Applications*; Wiley-VCH GmbH, 2001.
27. Enyedy, E. A.; Farkas, E.; Dömötör, O.; Santos, M. A. *J. Inorg. Biochem.* **2011**, *105*, 444.
28. Levine, R. L. *Clin. Chem.* **1977**, *23*, 2292.
29. Weisiger, R. A.; Ostrow, J. D.; Koehler, R. K.; Webster, C. C.; Mukerjee, P.; Pascolo, L.; Tiribelli, C. *J. Biol. Chem.* **2001**, *276*, 29953.
30. Mayer, M.; Meyer, B. *Angew. Chem., Int. Ed.* **1999**, *38*, 1784.
31. Verdonk, M. L.; Cole, J. C.; Hartshorn, M. J.; Murray, C. W.; Taylor, R. D. *Proteins* **2003**, *52*, 609.
32. Ghuman, J.; Zunszain, P. A.; Petitpas, I.; Bhattacharya, A. A.; Otagiri, M.; Curry, S. *J. Mol. Biol.* **2005**, *353*, 38.
33. Sabatini, A.; Vacca, A.; Gans, P. *Talanta* **1974**, *21*, 53.
34. Chasteen, N. D.; Grady, J. K.; Holloway, C. E. *Inorg. Chem.* **1986**, *25*, 2754.
35. Berman, H. M.; Westbrook, J.; Feng, Z.; Gilliland, G.; Bhat, T. N.; Weissig, H.; Shindyalov, I. N.; Bourne, P. E. *Nucleic Acids Res.* **2000**, *28*, 235.
36. *Maestro*, version 9.0; Schrödinger Inc: Portland, OR, 2009.